International Journal of
Molecular Sciences

MDPI

Article

Knockout of Purinergic P2Y$_6$ Receptor Fails to Improve Liver Injury and Inflammation in Non-Alcoholic Steatohepatitis

Kazuhiro Nishiyama [1], Kohei Ariyoshi [1], Akiyuki Nishimura [2,3], Yuri Kato [1], Xinya Mi [1], Hitoshi Kurose [1], Sang Geon Kim [4] and Motohiro Nishida [1,2,3,*]

1 Graduate School of Pharmaceutical Sciences, Kyushu University, Fukuoka 812-8582, Japan
2 National Institute for Physiological Sciences (NIPS), National Institutes of Natural Sciences, Okazaki 444-8787, Japan
3 Exploratory Research Center on Life and Living Systems (ExCELLS), National Institutes of Natural Sciences, Okazaki 444-8787, Japan
4 College of Pharmacy, Dongguk University-Seoul, Goyang-si 10326, Gyeonggi-Do, Republic of Korea
* Correspondence: nishida@phar.kyushu-u.ac.jp; Tel./Fax: +81-92-642-6556

Abstract: Nonalcoholic steatohepatitis (NASH) is a disease that progresses from nonalcoholic fatty liver (NAFL) and which is characterized by inflammation and fibrosis. The purinergic P2Y$_6$ receptor (P2Y$_6$R) is a pro-inflammatory G_q/G_{12} family protein-coupled receptor and reportedly contributes to intestinal inflammation and cardiovascular fibrosis, but its role in liver pathogenesis is unknown. Human genomics data analysis revealed that the liver P2Y$_6$R mRNA expression level is increased during the progression from NAFL to NASH, which positively correlates with inductions of C-C motif chemokine 2 (CCL2) and collagen type I α1 chain (Col1a1) mRNAs. Therefore, we examined the impact of P2Y$_6$R functional deficiency in mice crossed with a NASH model using a choline-deficient, L-amino acid-defined, high-fat diet (CDAHFD). Feeding CDAHFD for 6 weeks markedly increased P2Y$_6$R expression level in mouse liver, which was positively correlated with CCL2 mRNA induction. Unexpectedly, the CDAHFD treatment for 6 weeks increased liver weights with severe steatosis in both wild-type (WT) and P2Y$_6$R knockout (KO) mice, while the disease marker levels such as serum AST and liver CCL2 mRNA in CDAHFD-treated P2Y$_6$R KO mice were rather aggravated compared with those of CDAHFD-treated WT mice. Thus, P2Y$_6$R may not contribute to the progression of liver injury, despite increased expression in NASH liver.

Keywords: purinergic P2Y$_6$ receptor; nonalcoholic steatohepatitis; inflammation

Citation: Nishiyama, K.; Ariyoshi, K.; Nishimura, A.; Kato, Y.; Mi, X.; Kurose, H.; Kim, S.G.; Nishida, M. Knockout of Purinergic P2Y$_6$ Receptor Fails to Improve Liver Injury and Inflammation in Non-Alcoholic Steatohepatitis. *Int. J. Mol. Sci.* **2023**, *24*, 3800. https://doi.org/10.3390/ijms24043800

Academic Editor: Ronald Sluyter

Received: 27 December 2022
Revised: 10 February 2023
Accepted: 13 February 2023
Published: 14 February 2023

1. Introduction

Even if patients have no obvious drinking history, nonalcoholic fatty liver disease (NAFLD) is a liver illness that resembles alcoholic liver disease. The main contributing factor to the onset of NAFLD is obesity [1,2]. Nonalcoholic fatty liver (NAFL) and nonalcoholic steatohepatitis (NASH) are two symptoms of NAFLD. Triglyceride buildup is the cause of NAFL formation. NASH is an advanced type of NAFL, in which the liver tissue exhibits fibrosis comparable to alcoholic steatohepatitis and an influx of inflammatory cells [3]. It is generally accepted that inflammatory cell infiltration takes place first, followed by fibrosis, in terms of the evolution of the two conditions. According to epidemiology, NASH is linked to dyslipidemia, hypertension, fasting hyperglycemia, and metabolic syndrome [4]. The number of NAFL/NASH patients is increasing year by year, and the development of epoch-making preventive and therapeutic drugs is urgently needed [5].

Extracellular nucleosides and nucleotides are known as major damage-associated molecular patterns and mediate inflammation through stimulating a group of G-protein-coupled receptors (GPCRs) known as purinergic P2Y receptors (P2YRs) and purinergic P2X ion channels (P2XRs) [6,7]. Purinergic receptors are expressed in almost all mammalian tissues [8]. These receptors are also expressed in liver resident cells and play a

critical role in maintaining liver function [9,10]. Based on their G-protein selectivity and sequence similarity, P2YRs have been divided into two subfamilies: $P2Y_{12}$-like receptors ($P2Y_{12}R$, $P2Y_{13}R$, and $P2Y_{14}R$) share 45–50% sequence similarity and pair mostly with pertussis toxin-sensitive $G_{i/o}$, whereas $P2Y_1$-like receptors ($P2Y_1R$, $P2Y_2R$, $P2Y_4R$, $P2Y_6R$, and $P2Y_{11}R$) share 28–52% sequence homology [11]. Among them, we previously reported that $P2Y_6R$ couples with G_q and G_{12} family proteins and takes part in the signaling cascades that lead to pressure overload-induced cardiac remodeling, particularly to interstitial fibrosis [12]. Exposure of cardiomyocytes to mechanical stress the increased expression level of $P2Y_6R$ mRNA, and the pharmacological inhibition of $P2Y_6R$ prevents pressure overload-induced heart failure in mice [12]. By contrast, cardiomyocyte-specific overexpression of $P2Y_6R$ exacerbates pressure overload-induced heart failure [13]. We also reported that $P2Y_6R$ contributes to the progression of age-related hypertension and inflammatory bowel disease, and $P2Y_6R$ knockout mice show the prevention of tissue remodeling, including fibrosis and inflammation [14,15]. These results suggest a positive relationship between $P2Y_6R$ expression and the severity of tissue fibrosis and inflammation. In addition, $G\alpha_{12}$ levels are markedly diminished in liver biopsies from NAFLD patients, and $G\alpha_{12}$ overexpression induced by miR-16 dysregulation contributes to liver fibrosis by promoting autophagy in hepatic stellate cells [16]. In contrast, $G\alpha_{12}$ signaling is found to regulate sirtuin (SIRT) 1-dependent mitochondrial energy expenditure through hypoxia-inducible factor-1α-dependent ubiquitin-specific peptidase 22 induction, which leads to the stabilization of SIRT1 [17]. These reports strongly suggest that $P2Y_6R$-$G\alpha_{12}$ signaling is a plausible drug target for NASH.

In this study, we aim to clarify the involvement of $P2Y_6R$ signaling in the progression of NASH and to show whether $P2Y_6R$ becomes a new therapeutic target for NASH. Unexpectedly, however, we demonstrate that the suppression of $P2Y_6R$ signaling fails to improve the progression of liver injury using mice fed with the choline-deficient, L-amino acid-defined, high-fat diet (CDAHFD).

2. Results

2.1. Increase in mRNA Expression Levels of $P2Y_6R$, CCL2 and Col1a1 in NASH Patients

We searched open resources to investigate whether the mRNA expression levels of P2YRs and C-C motif chemokine 2 (CCL2), as inflammatory markers, and collagen type I alpha 1 chain (Col1a1), as a fibrosis marker, are altered in NASH patients. The mRNA expression levels of CCL2 and Col1a1 were increased in NASH patients' livers compared with NAFL patients' livers (Figure 1A). Among P2Y receptors, $P2Y_1R$, $P2Y_6R$, $P2Y_{11}R$, $P2Y_{13}R$, and $P2Y_{14}R$ were increased in NASH patients compared with NAFL patients (Figure 1A). The mRNA expression level of $P2Y_6R$ showed a positive correlation with the mRNA expression levels of CCL2 and Col1a1 (Figure 1B). These data suggested that the liver $P2Y_6R$ mRNA expression increases during the progression from NAFL to NASH.

2.2. Effects of $P2Y_6R$ Knockout on Body Status Changes Induced by CDAHFD

Next, to investigate whether the expression levels of $P2Y_6R$ and CCL2 are increased in a diet-induced NASH mouse model (CDAHFD), we measured the expression levels of $P2Y_6R$ and CCL2 in the liver. $P2Y_6R$ and CCL2 mRNA expression levels were increased in the liver of CDAHFD-fed mice compared to mice fed the standard (control) diet (Figure 2A). The mRNA expression level of $P2Y_6R$ showed a positive correlation with the mRNA expression level of CCL2 in mice liver (Figure 2B). The protein expression level of $P2Y_6R$ was increased in hepatocytes from mice fed with CDAHFD compared to those fed the control diet (Figure 2C). We examined the impact of $P2Y_6R$ functional deficiency in the diet-induced NASH model. It has been reported that mice fed with a normal diet gain body weight, while mice fed with CDAHFD maintain little or even slightly lose body weight [18]. CDAHFD-fed WT mice slightly lost body weight. The body weight of $P2Y_6R$ knockout (KO) mice fed with CDAHFD was changed in the same manner as occurred for WT mice fed with CDAHFD (Figure 2D). We confirmed that the food intake, water intake, and stool

numbers in P2Y$_6$R KO mice were similar to those in WT. Urine volume in P2Y$_6$R KO mice fed with CDAHFD was reduced compared to WT mice fed with CDAHFD (Figure 2E–H).

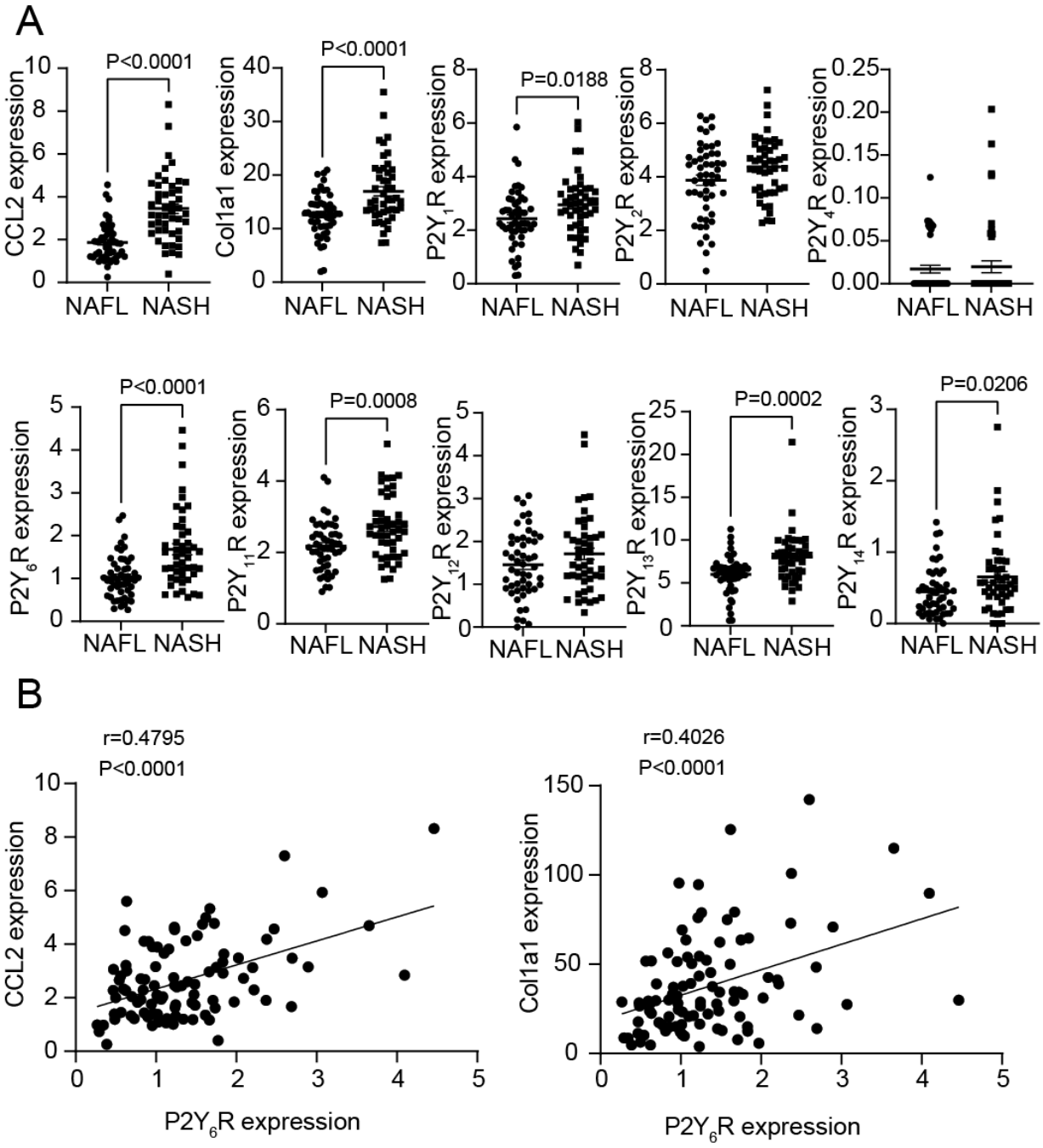

Figure 1. Increase in mRNA expression levels of P2Y$_6$R, CCL2 and Col1a1 in NASH patients. (**A**) The expression of CCL2, Col1a1, and P2Y receptors was analyzed in a Gene Expression Omnibus (GEO) dataset (GSE167523) containing the expression profile of the liver from NASH patients. (**B**) Correlation diagram between the expression levels of P2Y$_6$R and the expression levels of CCL2 and col1a1. Data are shown as the mean ± SEM. (NAFL; n = 51, NASH; n = 47) Student's t test (**A**). Pearson's product moment correlation coefficient (**B**).

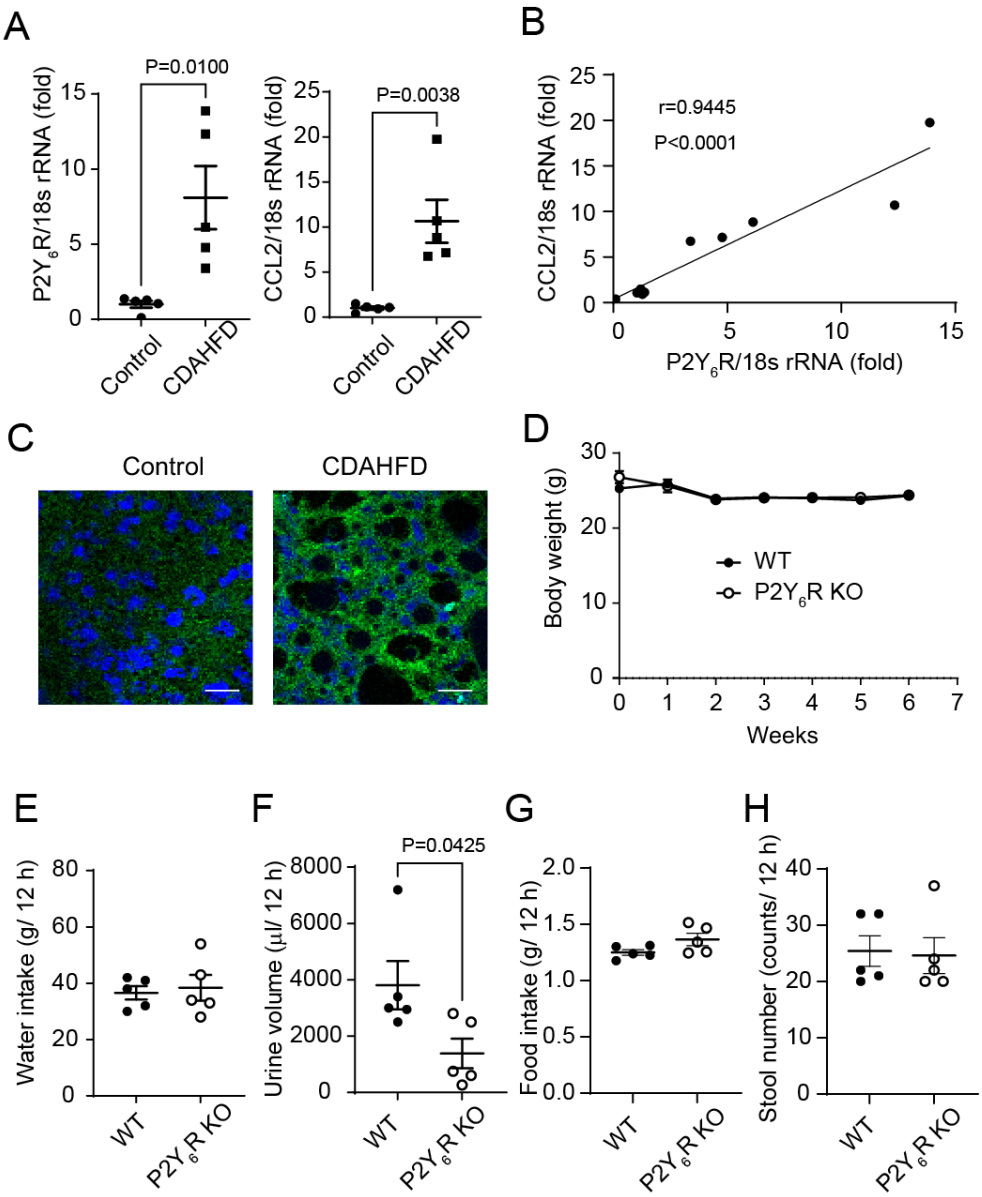

Figure 2. Effects of $P2Y_6R$ knockout on body status changes induced by CDAHFD. (**A**) The mRNA expression of $P2Y_6R$ and CCL2 in the livers of C57BL/6J mice fed with standard diet (control) or CDAHFD for 6 weeks ($n = 5$ in each group). (**B**) Correlation diagram between the expression levels of $P2Y_6R$ and the expression levels of CCL2 in mouse liver. (**C**) Immunohistological staining of $P2Y_6R$ in the liver of mice fed with standard diet or CDAHFD for 6 weeks. Scale bar: 40 μm. CDAHFD were fed to WT and $P2Y_6R$ KO mice for 6 weeks. (**D**) Body weight. (**E**) Water intake. (**F**) Urine volume. (**G**) Food intake. (**H**) Stool number. Data are shown as the mean ± SEM ($n = 5$ in each group). Student's *t* test (**A**,**F**). Pearson's product moment correlation coefficient (**B**).

2.3. Liver Weights and Serum Levels of AST and ALT

CDAHFD feeding increased liver weight in WT mice (Figure 3A). Liver weights in CDAHFD-fed $P2Y_6R$ KO mice were reduced in comparison to those in CDAHFD-fed WT mice (Figure 3A). To evaluate liver damage, we measured serum levels of liver-damaging enzymes such as aspartate aminotransferase (AST) and alanine aminotransferase (ALT) [19]. AST in $P2Y_6R$ KO mice fed with a CDAHFD diet was increased in comparison to WT mice fed with CDAHFD (Figure 3B). ALT in $P2Y_6R$ KO mice fed with a CDAHFD diet was increased in comparison to $P2Y_6R$ KO mice fed with the control diet (Figure 3C). These data suggested that the knockout of the $P2Y_6R$ aggravates CDAHFD-induced liver injury.

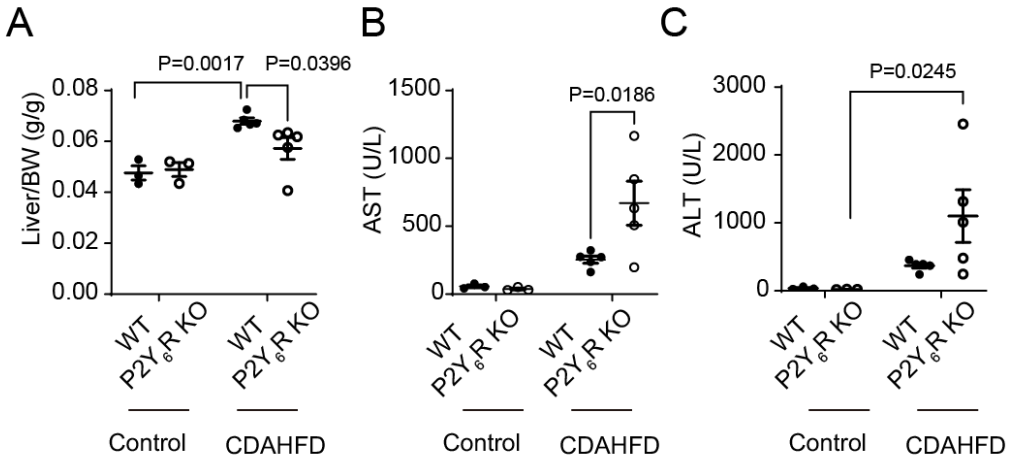

Figure 3. Liver weights and serum levels of AST and ALT in WT and $P2Y_6R$ KO mice fed with CDAHFD. (**A**) Liver weights. (**B**,**C**) Comparison of serum levels of AST (**B**) and ALT (**C**) among $P2Y_6R$ KO and WT mice. Data are shown as the mean ± SEM (control WT: $n = 3$, control $P2Y_6R$ KO: $n = 3$, CDAHFD WT: $n = 5$, CDAHFD $P2Y_6R$ KO: $n = 5$). Two-way ANOVA followed Sidak's multiple comparison test.

2.4. Liver Histology

We found that CDAHFD feeding caused predominantly middle droplet steatosis and inflammatory cell infiltration in the liver of WT mice and $P2Y_6R$ (Figure 4A). The severity of steatosis was similar in WT and $P2Y_6R$ KO mice fed with CDAHFD (Figure 4B). The infiltration of inflammatory cells was similar in CDAHFD-fed WT and $P2Y_6R$ KO mice (Figure 4A). These data suggested that a knockout of the $P2Y_6R$ does not affect CDAHFD-induced steatosis.

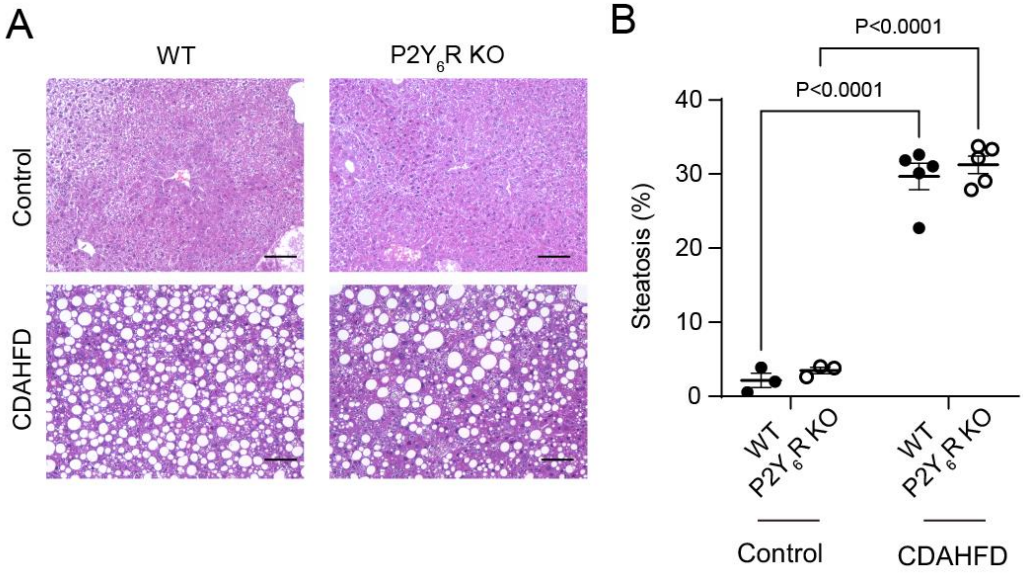

Figure 4. Effects of $P2Y_6R$ knockout on liver steatosis induced by CDAHFD. (**A**) H&E-stained images of liver sections. Scale bar: 100 μm. (**B**) Liver steatosis. Data are shown as the mean ± SEM (control WT: $n = 3$, control $P2Y_6R$ KO: $n = 3$, CDAHFD WT: $n = 5$, CDAHFD $P2Y_6R$ KO: $n = 5$). Two-way ANOVA followed Sidak's multiple comparison test.

2.5. Inflammation and Fibrosis of the Liver

CCL2 and interleukin-6 (IL-6) were analyzed as factors involved in the inflammation of the liver [20]. The mRNA expression level of CCL2, but not IL-6, in the liver of CDAHFD-fed $P2Y_6R$ KO mice was increased more than in the liver of CDAHFD-fed WT

mice (Figure 5A,B). TGFβ1 and Col1a1 were analyzed as factors involved in liver fibrosis. CDAHFD feeding increased the expression levels of both fibrotic factors in the liver of WT mice and P2Y$_6$R mice. Both TGFβ1 and Col1a1 were similarly expressed in WT and P2Y$_6$R KO mice fed with CDAHFD (Figure 5C,D). These data suggested that a knockout of the P2Y$_6$R aggravates CDAHFD-induced inflammation but not fibrosis.

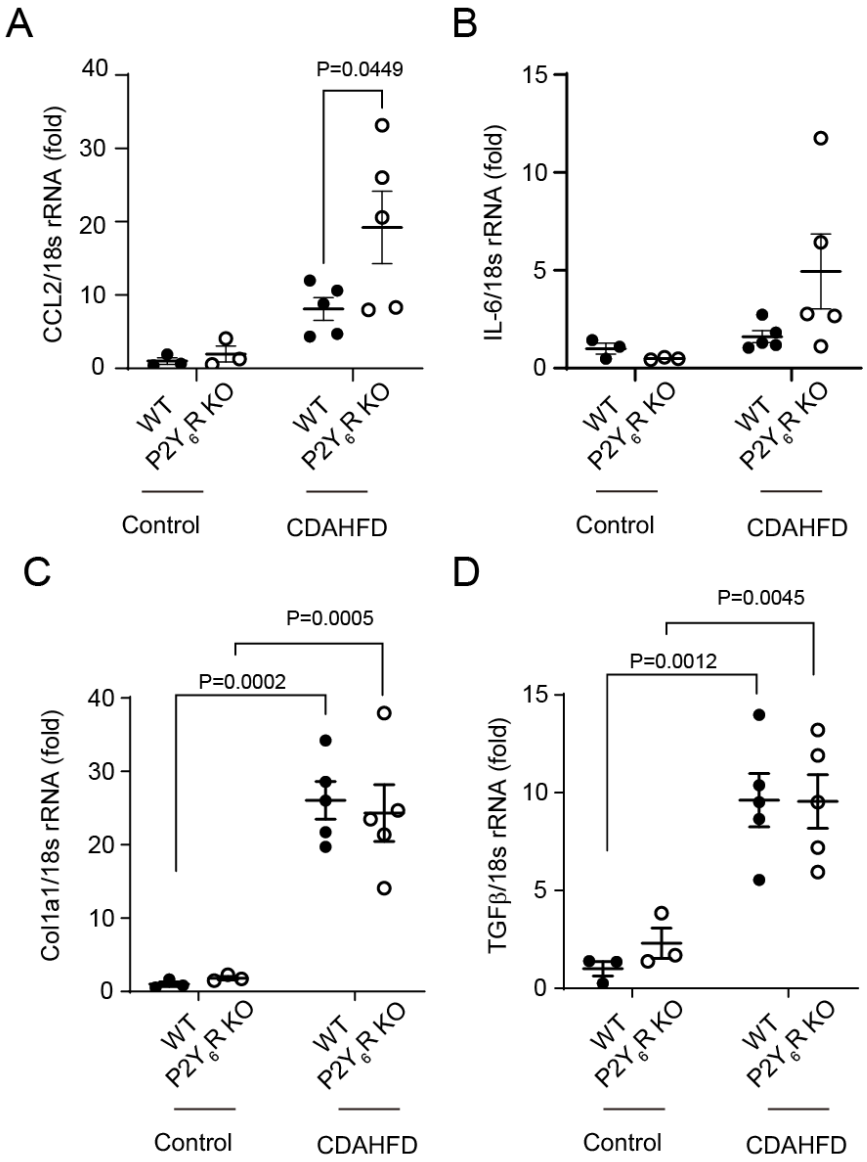

Figure 5. Knockout of P2Y$_6$R accelerated expression of liver inflammation markers induced by CDAHFD feeding. Expression of CCL2 (**A**), IL-6 (**B**), Col1a1 (**C**), and TGFβ (**D**) in liver were quantified by real-time qPCR. Data are shown as the mean ± SEM (control WT: n = 3, control P2Y$_6$R KO: n = 3, CDAHFD WT: n = 5, CDAHFD P2Y$_6$R KO: n = 5). Two-way ANOVA followed Sidak's multiple comparison test.

3. Discussion

P2Y$_6$R is expressed in various cell types. P2Y$_6$R KO mice are alive and do not differ in growth or fertility from its littermate WT mice, but show remarkable phenotypes in several stress conditions [21]. The synthesis of inositol 1,4,5-trisphosphate induced by UDP stimulation was eliminated in thioglycolate-elicited mouse macrophages, demonstrating that P2Y$_6$R is the only UDP-responsive receptor present in macrophages. UDP-dependent enhanced responsiveness to LPS stimulation was abolished in P2Y$_6$R KO macrophages [21]. Endothelial-dependent vasorelaxation, induced by UDP stimulation, and contraction,

induced by UDP upon the inhibition of endothelial nitric oxide synthase, were abolished in $P2Y_6R$-deficient aortas [21]. $P2Y_6R$ KO mice did not display atherosclerosis, vascular inflammation, age-related hypertension and intestinal inflammation [14,15,22]. Compared to wild-type mice, $P2Y_6R$ KO mice show a significant resistance to the skin papilloma-inducing effects of 7,12-dimethylbenz[a]anthracene/12-O-tetradecanoylphorbol-13-acetate [23]. $P2Y_6R$ deletion prevented the neuronal and memory loss caused by tubulin-associated unit causes [24].

Hepatocytes, immune cells such as Kupffer cells and macrophages, and hepatic stellate cells are involved in the progression of NASH [25]. According to the database [26,27], $P2Y_6R$ is highly expressed in immune cells such as macrophages. $P2Y_6R$ regulates phagocytosis and the production of inflammatory cytokines in macrophages or microglia [22,28,29]. $P2Y_6R$ is also expressed in hepatic stellate cells (HSCs) [30]. Treatment of activated HSCs with UDP (native $P2Y_6R$ agonist) tripled the mRNA levels of procollagen-1 [30]. The inhibition of $P2Y_6R$ ameliorates the pathology of the alcoholic steatohepatitis (ASH) model [31]. $P2Y_6R$ deficiency in adipocytes protects mice from diet-induced obesity due to enhanced energy expenditure and reduced inflammation, with white adipose tissue browning also being reported [32]. These reports suggest that $P2Y_6R$ may contribute to the progression of liver inflammation and fibrosis. However, we demonstrated that the degree of liver fibrosis in $P2Y_6R$ KO mice fed with CDAHFD was similar to that in WT mice with CDAHFD, but inflammation and liver injury were rather exacerbated in $P2Y_6R$ KO mice. $P2Y_6R$ KO mice have been shown to exhibit different phenotypes depending on the environment and experimental site, even with the same inflammation model [15,33]. In addition, knockout of $P2Y_6R$ in muscle has been shown to increase insulin resistance [32]. Liver weights in $P2Y_6R$ KO mice fed with CDAHFD were reduced in comparison to WT mice fed with CDAHFD. The liver weight increases in proportion to the severity of fatty liver present in the CDAHFD model, but it has been reported that the liver weight decreases when fibrosis also progresses [3,34]. The mRNA expression level of CCL2 in $P2Y_6R$ KO mice fed with CDAHFD was increased compared to that in WT mice fed with CDAHFD. These data suggest that $P2Y_6R$ knockout slightly promotes liver fibrosis and inflammation. Urine volume in $P2Y_6R$ KO mice fed with CDAHFD was reduced compared to that in WT mice fed with CDAHFD. It has been reported that $P2Y_6R$ KO mice display more frequent micturition, with smaller bladder capacity compared to WT mice [35]. $P2Y_6R$ is also expressed in the kidney [26,27], but its physiological role is unclear. In addition, $P2Y_6R$ contributes to the pathogenesis of heart failure [12,13] and hypertension [14]. CDAHFD may stimulate $P2Y_6R$ signaling in the cardiovascular and renal tissues, causing the difference in urine output between $P2Y_6R$ KO and WT. Future investigations using tissue-specific $P2Y_6R$ KO mice are necessary to identify which cells are regulated by $P2Y_6R$ in the pathogenesis of NASH.

We showed that among the P2Y subtypes, $P2Y_1R$, $P2Y_6R$, $P2Y_{11}R$, $P2Y_{13}R$, and $P2Y_{14}R$ are increased in patients with NASH compared with patients with NAFL. Among them, $P2Y_6R$ showed the best positive correlation with CCL2 and Col1a1. These data suggest that $P2Y_6R$ expression level is increased according to the degree of inflammation and fibrosis. Infiltration of inflammatory cells with high $P2Y_6R$ expression may contribute to elevated $P2Y_6R$ expression in the NASH liver. Since the expression of $P2Y_6R$ is also increased by LPS [36], its expression is regulated in response to inflammation at the transcription level. On the other hand, we previously reported that $P2Y_6R$ proteins are internalized and degraded by cysteine modification by electrophiles and nitric oxide [15]. Oxidative stress is also known to contribute to the pathogenesis of NASH [4]. In the future, it is necessary to confirm the expression level and localization of $P2Y_6R$ at the protein level, including not only regulation of transcriptional level but also post-translational modification in patients, to clarify the role of $P2Y_6R$ in NASH pathogenesis.

Smoking is positively correlated with NAFLD [37]. Involvement of intestinal nicotine concentration and intestinal microbiota has been reported [37]. On the other hand, it is also known that smoking components contain large amounts of electrophilic substances, such as aldehydes [38]. It is also known that smoking causes oxidative stress. Therefore,

the internalization and degradation of $P2Y_6R$ by smoking may exacerbate the pathology of NASH. Conversely, there is an epidemiological report that cigarette smoke suppresses the risk of onset, progression, and recurrence of ulcerative colitis (UC) [39]. We recently reported that post-translational modification of cysteine in the intracellular 3rd loop of $P2Y_6R$ through covalent binding with electrophilic molecules promotes redox-dependent (β-arrestin-independent) $P2Y_6R$ internalization, which contributes to the attenuation of UC progression in mice [15]. As smoking aldehydes are environmental electrophiles, smoking aldehydes may increase the risk of NAFLD severity by promoting internalization and degradation of $P2Y_6R$.

P2YRs are GPCRs that have been further divided into two subfamilies based on G-protein selectivity and sequence similarity. Among the P2YRs, $P2Y_2R$ is known to promote high-fat diet (HFD)-induced hepatic steatosis [40]. Platelets control liver tumor growth through $P2Y_{12}R$-dependent CD40L release in NAFLD [41]. Another study revealed that mice lacking $P2Y_{14}R$ selectively in adipocytes were protected from obesity and displayed reduced liver weight compared to HFD control mice [42]. Reduced obesity and hepatic steatosis further contributed to improved insulin sensitivity in the liver of adipocyte-$P2Y_{14}R$ KO mice [42]. On the other hand, $P2Y_6R$ is known to couple with $G_{12/13}$. G_{12}-mediated signaling is known to regulate hepatic lipid metabolism, and G_{12}-knockout mice are reported to display aggravated fatty liver [17]. We showed that $P2Y_6R$ signaling, despite its elevated expression, is not involved in pathogenesis and production of inflammatory markers in fatty liver. $P2Y_6R$ may maintain liver homeostasis through G_{12} signaling.

Other purinergic receptors, namely P2XRs and adenosine receptors (ARs), have also been reportedly involved in NASH/NALFD progression. P2X7R expression level was elevated in hepatocytes, Kupffer cells, and liver sinusoidal endothelial cells of NASH model mice [43]. In mice given carbon tetrachloride (CCl4) and HFD, the deficiency of $P2X_7R$ prevents inflammation, fibrosis and hepatocyte apoptosis [43,44]. $P2X_7R$ activation on Kupffer cells enhances TNFα and monocyte chemotactic protein-2 (MCP-2) production in HFD mice treated with CCl4 [44]. These findings imply that $P2X_7R$ antagonism might be a beneficial strategy for the treatment of NASH. Adenosine A_1AR expression in the liver of streptozotocin (STZ)-induced diabetic rats was elevated [45]. A separate study, however, asserted that A_1AR expression remained unchanged while $A_{2A}AR$ and $A_{3A}R$ receptor levels were dramatically elevated in STZ-treated rat liver [46]. $A_{2A}AR$ activation reduces inflammation [47,48], but its absence increases pro-inflammatory responses [49]. Furthermore, in mice, the absence of whole-body $A_{2A}AR$ exacerbated HFD-induced NAFLD and hepatic inflammation [50]. As a result, $A_{2A}AR$ deficiency in hepatocytes and macrophages contributed to increased inflammation [50]. The anti-inflammatory activity of $A_{2A}AR$ was also observed in a study of the methionine- and choline-deficient (MCD)-induced NASH animal model. The $A_{2A}AR$ KO mice, treated with the MCD-NASH model show a larger body weight, increased liver inflammation, and more severe hepatic steatosis than the control mice [51]. The biological effect of $A_{2A}R$ activation in reducing inflammation caused by lipotoxicity can lead to the protection of mouse liver against NASH progression [52,53]. $A_{2B}AR$ has also been shown to have an important function in the regulation of fatty liver disease. $A_{2B}AR$ deficiency protected mice from hepatic steatosis and the formation of fatty liver [54]. In diabetic KKA^Y mice, inhibiting $A_{2B}AR$ with the specific antagonist ATL-801 reduced glucose production during hyperinsulinemic-euglycemic clamp tests [55]. According to some studies, the activation of $A_{2B}AR$ suppressed lipogenic genes such as sterol regulatory element-binding protein-1 (SREBP-1). The $A_{2B}AR$ KO mice fed with HFD caused hepatic steatosis with increased plasma triglyceride and cholesterol levels [56]. Furthermore, hepatic $A_{2B}AR$ overexpression and activation lowered lipid production in the liver and enhanced whole-body metabolism [56]. On a typical diet, $A_{2B}AR$ KO mice lost weight and had enhanced de novo lipogenesis, resulting in raised liver triglyceride levels. Increased glucokinase and fatty acid synthase mRNA levels revealed poor lipid metabolism in the liver of $A_{2B}AR$ KO mice [57]. The $A_{2B}AR$ KO mice fed with HFD show poor glucose tolerance and insulin sensitivities [58]. WT mice treated with an $A_{2B}AR$ agonist/partial

agonist, BAY60-6553, reportedly enhance glucose and insulin tolerance as well as lower fasting blood glucose levels [58]. These reports suggest that adenosine signaling through A_{2A}AR and/or A_{2B}AR activations will be a promising therapeutic target for the treatment of liver disorders.

Recent research has underlined the significance of the A_3AR in NAFLD/NASH. A_3AR expression was reduced 1.9-fold in NAFLD patients' livers compared to controls, indicating possible involvement by the receptor in NAFLD pathogenesis [59]. A_3AR deficiency in mice given an HFD increased the expression of genes implicated in hepatic inflammation and steatosis [59]. The researchers demonstrated that an $A3_A$R agonist prodrug (MRS7476) protected the STAM mouse model from the development of NASH [59]. MRS7476's two succinyl ester groups significantly improve its water solubility and are most likely cleaved in the gut rather than at the site of action. Another study found that the A_3AR agonist Cl-IB-MECA (namodenoson) was effective in treating NASH in mice [60]. The drug namodenoson is currently in Phase 2 clinical trials for NASH therapeutics [10].

In this study, we show that $P2Y_6$R knockout slightly promotes NASH pathology. However, we have not investigated whether $P2Y_6$R activation inhibits the progression of NASH. UDPβS and Up3U are likewise $P2Y_6$R agonists [61]. Several potent and selective agonists for this receptor have been discovered, including 3-phenacyl-UDP (PSB-0474), 5-iodo-UDP (MRS2693), α,β-methylene-UDP (MRS2782), INS48823, and 5-O-methyl-UDPA [61]. Several analogues of boranophosphates are significantly more active at the $P2Y_6$R [61]. In the future, it will be necessary to examine whether such various $P2Y_6$R agonists suppress the pathological progression of NASH.

A limitation of this study is that almost all experiments were analyzed using NASH/NAFLD model mice, when the role of $P2Y_6$R in human NASH pathogenesis might in fact differ from that in mice. In this study, the CDAHFD model was used as the NASH model [18]. One of the most frequently utilized techniques in NASH research is the MCD model, which involves providing a diet low in both methionine and choline. Because methionine and choline are required for the hepatic secretion of triglycerides in the form of very low-density lipoproteins (VLDL), lipid export from the liver to peripheral tissues may be impaired in these models due to the defective incorporation of triglycerides into apolipoprotein B (ApoB), or reduced ApoB synthesis or excretion. The phenotype caused by the MCD diet includes macrovesicular steatosis, hepatocellular apoptosis, inflammation, oxidative stress, and fibrosis [62]. One disadvantage for using the MCD model to promote NASH development is that these mice will cause a significant systemic weight loss [63,64]. CDAHFD model may be a mouse model of rapidly progressive liver fibrosis and could be potentially useful for better understanding human NASH disease as well as in the development of efficient therapies for this condition. However, the pathogenesis and etiology of CDAHFD-fed mice do not necessarily match those of human patients with NASH. Future studies using induced pluripotent stem cell (iPS cell) and organoids will be necessary for elucidating the role(s) of purinergic signaling in human NASH.

In conclusion, we demonstrated using an online database that $P2Y_6$R expression level is increased in NAFLD patients according to the degree of inflammation and fibrosis. We also revealed using NASH model mice that knockout of the $P2Y_6$R fails to improve (but instead aggravates) liver injury and inflammation. Our findings will prompt reconsideration of $P2Y_6$R-G_{12} signaling as a therapeutic strategy for NASH.

4. Materials and Methods

4.1. GEO Datasets Analysis

GEO RNA-Sequencing Experiments Interactive Navigator [65] was used to retrieve normalized transcript levels from the GEO dataset GSE167523 [66]. We analyzed the transcript levels of P2YRs, CCL2 and Col1a1 in NAFL and NASH patients.

4.2. Animals

All animal care and experimental procedures used in this study were approved by the ethics committees at the Animal Care and Use Committee of Kyushu University. Systemic $P2Y_6R$ KO mice were backcrossed onto C57BL/6J mice background, as described previously [13–15]. We used $P2Y_6R$ KO and cohoused littermates as WT (8–11 weeks old, male). Animals were maintained under a 12 h/12 h light/dark cycle.

4.3. Diet-Induced NASH Model

We fed male mice CDAHFD (Research Diets Inc., New Brunswick, NJ, USA, Cat# A06071302) or a control diet (Research Diets Inc., New Brunswick, NJ, USA, Cat# A06071314) for 6 weeks [18]. After 6 weeks, we euthanized all mice under isoflurane anesthesia. We took the liver from mice and measured liver weights. We collected blood samples from the caudal vena cava and centrifuged these at 10,000× *g* for 10 min.

4.4. Immunohistochemistry

For tissue sections, the liver tissue was fixed by 4% paraformaldehyde. Frozen sections (5 µm thick) were cut and prepared for immunofluorescent staining [67]. The expression of $P2Y_6R$ was detected using rabbit anti-$P2Y_6R$ antibodies (#APR011: Alomone Labs, Jerusalem, Israel). The immunoreactivity of $P2Y_6R$ was detected using an Alexa Fluor 488-labeled goat anti-rabbit IgG antibody (#A-11008: ThermoFisher Scientific, Waltham, MA, USA). Non-specific immunoreactivity was blocked with 10% normal goat serum, 1% BSA, and 0.3% Triton X-100 in PBS. After incubation with the secondary antibody, images were captured using a confocal laser-scanning microscope (LSM900, Zeiss, Oberkochen, Germany).

4.5. Serum Biochemical Analysis

We measured serum levels of AST and ALT by using Fuji Dry-Chem NX5000 (FUJIFILM Medical, Tokyo, Japan) [2].

4.6. Histological Evaluation of the Liver

We fixed the liver with 10% neutral buffered formalin and embedded these in paraffin. We performed hematoxylin and eosin (H&E) staining, as previously described [2]. We quantified empty envelopes using ImageJ and evaluated as steatosis [2].

4.7. RNA Isolation and qPCR

We extracted total RNA from the liver, as previously described [67]. The RNA was used to synthesize complementary DNA using ReverTra Ace (Toyobo, Osaka, Japan). We performed qPCR as previously described [67,68]. Primer sequences used are summarized in Supplementary Table S1. To normalize cDNA levels, 18 s rRNA expression was used as an endogenous control.

4.8. Statistics

Statistical analysis were performed by using GraphPad Prism 9.0 (GraphPad Software, LaJolla, CA, USA) [2]. All results were expressed as mean ± SEM from at least 3 independent experiments. Statistical comparisons were determined using two-tailed Student's *t* tests (for two groups) or using the one-way ANOVA method with Tukey's post hoc test (for three or more groups).

Supplementary Materials: The following supporting information can be downloaded at: https://www.mdpi.com/article/10.3390/ijms24043800/s1.

Author Contributions: M.N. and K.N. designed the research and wrote the paper; K.N., K.A., A.N., Y.K. and X.M. performed experiments; K.N., K.A., A.N., Y.K., H.K., S.G.K. and X.M. analyzed and interpreted data; M.N. edited the paper. All authors have read and agreed to the published version of the manuscript.

Funding: This study was supported by grants from JST CREST Grant Number JPMJCR2024 (20348438), JSPS KAKENHI (22K06630, 22H04814 to K.N. and 21H05269, 22H02772 to M.N.), and the National Research Foundation of Korea (NRF) funded by the Korean government (MSIP) (2017K1A1A2004511).

Institutional Review Board Statement: All animal studies were conducted according to the guidelines concerning the care and handling of experimental animals, and approved by the ethics committees at the National Institutes of Natural Sciences or the Animal Care and Use Committee, Kyushu University (protocol code: A20-250-0 approved on 29 September 2020).

Informed Consent Statement: Not applicable.

Data Availability Statement: Not applicable.

Acknowledgments: We appreciate the technical assistance from the Research Support Center, Research Center for Human Disease Modeling, Kyushu University Graduate School of Medical Sciences.

Conflicts of Interest: The authors declare no conflict of interest.

References

1. Baratta, F.; D'Erasmo, L.; Bini, S.; Pastori, D.; Angelico, F.; Del Ben, M.; Arca, M.; Di Costanzo, A. Heterogeneity of non-alcoholic fatty liver disease (NAFLD): Implication for cardiovascular risk stratification. *Atherosclerosis* **2022**, *357*, 51–59. [CrossRef] [PubMed]
2. Nishiyama, K.; Toyama, C.; Kato, Y.; Tanaka, T.; Nishimura, A.; Nagata, R.; Mori, Y.; Nishida, M. Deletion of TRPC3 or TRPC6 fails to attenuate the formation of inflammation and fibrosis in non-alcoholic steatohepatitis. *Biol. Pharm. Bull.* **2021**, *44*, 431–436. [CrossRef] [PubMed]
3. Azuma, Y.T.; Fujita, T.; Izawa, T.; Hirota, K.; Nishiyama, K.; Ikegami, A.; Aoyama, T.; Ike, M.; Ushikai, Y.; Kuwamura, M.; et al. Il-19 contributes to the development of nonalcoholic steatohepatitis by altering lipid metabolism. *Cells* **2021**, *10*, 3513. [CrossRef] [PubMed]
4. Takaki, A.; Kawai, D.; Yamamoto, K. Multiple hits, including oxidative stress, as pathogenesis and treatment target in non-alcoholic steatohepatitis (NASH). *Int. J. Mol. Sci.* **2013**, *14*, 20704–20728. [CrossRef]
5. Younossi, Z.M.; Golabi, P.; de Avila, L.; Paik, J.M.; Srishord, M.; Fukui, N.; Qiu, Y.; Burns, L.; Afendy, A.; Nader, F. The global epidemiology of NAFLD and NASH in patients with type 2 diabetes: A systematic review and meta-analysis. *J. Hepatol.* **2019**, *71*, 793–801. [CrossRef]
6. Jacobson, K.A.; Delicado, E.G.; Gachet, C.; Kennedy, C.; von Kügelgen, I.; Li, B.; Miras-Portugal, M.T.; Novak, I.; Schöneberg, T.; Perez-Sen, R.; et al. Update of P2Y receptor pharmacology: IUPHAR Review 27. *Br. J. Pharm.* **2020**, *177*, 2413–2433. [CrossRef]
7. Rotondo, J.C.; Mazziotta, C.; Lanzillotti, C.; Stefani, C.; Badiale, G.; Campione, G.; Martini, F.; Tognon, M. The Role of Purinergic P2X7 Receptor in Inflammation and Cancer: Novel Molecular Insights and Clinical Applications. *Cancers* **2022**, *14*, 1116. [CrossRef]
8. Li, L.; Liu, J.; Xu, A.; Heiduschka, P.; Eter, N.; Chen, C. Expression of purinergic receptors on microglia in the animal model of choroidal neovascularisation. *Sci. Rep.* **2021**, *11*, 12389. [CrossRef]
9. Daré, B.L.; Ferron, P.J.; Gicquel, T. The purinergic p2x7 receptor-nlrp3 inflammasome pathway: A new target in alcoholic liver disease? *Int. J. Mol. Sci.* **2021**, *22*, 2139. [CrossRef]
10. Jain, S.; Jacobson, K.A. Purinergic Signaling in Liver Pathophysiology. *Front. Endocrinol.* **2021**, *12*, 718429. [CrossRef]
11. Nishimura, A.; Sunggip, C.; Oda, S.; Numaga-Tomita, T.; Tsuda, M.; Nishida, M. Purinergic P2Y receptors: Molecular diversity and implications for treatment of cardiovascular diseases. *Pharmacol. Ther.* **2017**, *180*, 113–128. [CrossRef]
12. Nishida, M.; Sato, Y.; Uemura, A.; Narita, Y.; Tozaki-Saitoh, H.; Nakaya, M.; Ide, T.; Suzuki, K.; Inoue, K.; Nagao, T.; et al. P2Y6 receptor-Gα12/13 signalling in cardiomyocytes triggers pressure overload-induced cardiac fibrosis. *EMBO J.* **2008**, *27*, 3104–3115. [CrossRef]
13. Shimoda, K.; Nishimura, A.; Sunggip, C.; Ito, T.; Nishiyama, K.; Kato, Y.; Tanaka, T.; Tozaki-Saitoh, H.; Tsuda, M.; Nishida, M. Modulation of P2Y6R expression exacerbates pressure overload-induced cardiac remodeling in mice. *Sci. Rep.* **2020**, *10*, 13926. [CrossRef]
14. Nishimura, A.; Sunggip, C.; Tozaki-Saitoh, H.; Shimauchi, T.; Numaga-Tomita, T.; Hirano, K.; Ide, T.; Boeynaems, J.M.; Kurose, H.; Tsuda, M.; et al. Purinergic P2Y6 receptors heterodimerize with angiotensin AT1 receptors to promote angiotensin II-induced hypertension. *Sci. Signal.* **2016**, *9*, ra7. [CrossRef]
15. Nishiyama, K.; Nishimura, A.; Shimoda, K.; Tanaka, T.; Kato, Y.; Shibata, T.; Tanaka, H.; Kurose, H.; Azuma, Y.T.; Ihara, H.; et al. Redox-dependent internalization ofthe purinergic P2Y6 receptor limits colitis progression. *Sci. Signal.* **2022**, *15*, eabj0644. [CrossRef]
16. Kim, K.M.; Han, C.Y.; Kim, J.Y.; Cho, S.S.; Kim, Y.S.; Koo, J.H.; Lee, J.M.; Lim, S.C.; Kang, K.W.; Kim, J.S.; et al. Gα12 overexpression induced by miR16 dysregulation contributes to liver fibrosis by promoting autophagy in hepatic stellate cells. *J. Hepatol.* **2018**, *68*, 493–504. [CrossRef]
17. Kim, T.H.; Yang, Y.M.; Han, C.Y.; Koo, J.H.; Oh, H.; Kim, S.S.; You, B.H.; Choi, Y.H.; Park, T.S.; Lee, C.H.; et al. Gα12 ablation exacerbates liver steatosis and obesity by suppressing USP22/SIRT1-regulated mitochondrial respiration. *J. Clin. Investig.* **2018**, *128*, 5587–5602. [CrossRef]

18. Matsumoto, M.; Hada, N.; Sakamaki, Y.; Uno, A.; Shiga, T.; Tanaka, C.; Ito, T.; Katsume, A.; Sudoh, M. An improved mouse model that rapidly develops fibrosis in non-alcoholic steatohepatitis. *Int. J. Exp. Pathol.* **2013**, *94*, 93–103. [CrossRef]
19. Ozer, J.; Ratner, M.; Shaw, M.; Bailey, W.; Schomaker, S. The current state of serum biomarkers of hepatotoxicity. *Toxicology* **2008**, *245*, 194–205. [CrossRef]
20. Haukeland, J.W.; Damås, J.K.; Konopski, Z.; Løberg, E.M.; Haaland, T.; Goverud, I.; Torjesen, P.A.; Birkeland, K.; Bjøro, K.; Aukrust, P. Systemic inflammation in nonalcoholic fatty liver disease is characterized by elevated levels of CCL2. *J. Hepatol.* **2006**, *44*, 1167–1174. [CrossRef]
21. Bar, I.; Guns, P.J.; Metallo, J.; Cammarata, D.; Wilkin, F.; Boeynams, J.M.; Bult, H.; Robaye, B. Knockout mice reveal a role for P2Y6 receptor in macrophages, endothelial cells, and vascular smooth muscle cells. *Mol. Pharmacol.* **2008**, *74*, 777–784. [CrossRef] [PubMed]
22. Stachon, P.; Peikert, A.; Michel, N.A.; Hergeth, S.; Marchini, T.; Wolf, D.; Dufner, B.; Hoppe, N.; Ayata, C.K.; Grimm, M.; et al. P2Y6 deficiency limits vascular inflammation and atherosclerosis in mice. *Arterioscler. Thromb. Vasc. Biol.* **2014**, *34*, 2237–2245. [CrossRef]
23. Xu, P.; Wang, C.; Xiang, W.; Liang, Y.; Li, Y.; Zhang, X.; Guo, C.; Liu, M.; Shi, Y.; Ye, X.; et al. P2RY6 Has a Critical Role in Mouse Skin Carcinogenesis by Regulating the YAP and β-Catenin Signaling Pathways. *J. Investig. Dermatol.* **2022**, *142*, 2334–2342.e8. [CrossRef] [PubMed]
24. Puigdellívol, M.; Milde, S.; Vilalta, A.; Cockram, T.O.J.; Allendorf, D.H.; Lee, J.Y.; Dundee, J.M.; Pampuščenko, K.; Borutaite, V.; Nuthall, H.N.; et al. The microglial P2Y6 receptor mediates neuronal loss and memory deficits in neurodegeneration. *Cell Rep.* **2021**, *37*, 110148. [CrossRef]
25. Caligiuri, A.; Gentilini, A.; Marra, F. Molecular pathogenesis of NASH. *Int. J. Mol. Sci.* **2016**, *17*, 1575. [CrossRef] [PubMed]
26. The Human Protein Atlas. Available online: https://www.proteinatlas.org/ (accessed on 25 December 2022).
27. Karlsson, M.; Zhang, C.; Méar, L.; Zhong, W.; Digre, A.; Katona, B.; Sjöstedt, E.; Butler, L.; Odeberg, J.; Dusart, P.; et al. A single–cell type transcriptomics map of human tissues. *Sci. Adv.* **2021**, *7*, eabh2169. [CrossRef]
28. Zhang, Z.; Wang, Z.; Ren, H.; Yue, M.; Huang, K.; Gu, H.; Liu, M.; Du, B.; Qian, M. P2Y6 agonist uridine 5′-diphosphate promotes host defense against bacterial infection via monocyte chemoattractant protein-1—mediated monocytes/macrophages recruitment. *J. Immunol.* **2011**, *186*, 5376–5387. [CrossRef]
29. Koizumi, S.; Shigemoto-Mogami, Y.; Nasu-Tada, K.; Shinozaki, Y.; Ohsawa, K.; Tsuda, M.; Joshi, B.V.; Jacobson, K.A.; Kohsaka, S.; Inoue, K. UDP acting at P2Y6 receptors is a mediator of microglial phagocytosis. *Nature* **2007**, *446*, 1091–1095. [CrossRef]
30. Dranoff, J.A.; Ogawa, M.; Kruglov, E.A.; Gaça, M.D.A.; Sévigny, J.; Robson, S.C.; Wells, R.G. Expression of P2Y nucleotide receptors and ectonucleotidases in quiescent and activated rat hepatic stellate cells. *Am. J. Physiol.-Gastrointest. Liver Physiol.* **2004**, *287*, G417–G424. [CrossRef]
31. Yuan, F.; Cai, J.N.; Dai, M.; Lv, X. Inhibition of P2Y6 receptor expression in Kupffer cells alleviates alcoholic steatohepatitis in mice. *Int. Immunopharmacol.* **2022**, *109*, 108909. [CrossRef]
32. Jain, S.; Pydi, S.P.; Toti, K.S.; Robaye, B.; Idzko, M.; Gavrilova, O.; Wess, J.; Jacobson, K.A. Lack of adipocyte purinergic P2Y6 receptor greatly improves whole body glucose homeostasis. *Proc. Natl. Acad. Sci. USA* **2020**, *117*, 30763–30774. [CrossRef]
33. Salem, M.; El Azreq, M.A.; Pelletier, J.; Robaye, B.; Aoudjit, F.; Sévigny, J. Exacerbated intestinal inflammation in P2Y6 deficient mice is associated with Th17 activation. *Biochim. Biophys. Acta Mol. Basis Dis.* **2019**, *1865*, 2595–2605. [CrossRef]
34. Lu, Y.; Su, X.; Zhao, M.; Zhang, Q.; Liu, C.; Lai, Q.; Wu, S.; Fang, A.; Yang, J.; Chen, X.; et al. Comparative RNA-sequencing profiled the differential gene expression of liver in response to acetyl-CoA carboxylase inhibitor GS-0976 in a mouse model of NASH. *PeerJ* **2019**, *7*, e8115. [CrossRef]
35. Kira, S.; Yoshiyama, M.; Tsuchiya, S.; Shigetomi, E.; Miyamoto, T.; Nakagomi, H.; Shibata, K.; Mochizuki, T.; Takeda, M.; Koizumi, S. P2Y6-deficiency increases micturition frequency and attenuates sustained contractility of the urinary bladder in mice. *Sci. Rep.* **2017**, *7*, 771. [CrossRef]
36. Yang, X.; Lou, Y.; Liu, G.; Wang, X.; Qian, Y.; Ding, J.; Chen, S.; Xiao, Q. Microglia P2Y6 receptor is related to Parkinson's disease through neuroinflammatory process. *J. Neuroinflamm.* **2017**, *14*, 38. [CrossRef]
37. Chen, B.; Sun, L.; Zeng, G.; Shen, Z.; Wang, K.; Yin, L.; Xu, F.; Wang, P.; Ding, Y.; Nie, Q.; et al. Gut bacteria alleviate smoking-related NASH by degrading gut nicotine. *Nature* **2022**, *610*, 562–568. [CrossRef]
38. Ogunwale, M.A.; Li, M.; Ramakrishnam Raju, M.V.; Chen, Y.; Nantz, M.H.; Conklin, D.J.; Fu, X.A. Aldehyde Detection in Electronic Cigarette Aerosols. *ACS Omega* **2017**, *2*, 1207–1214. [CrossRef]
39. Mahid, S.S.; Minor, K.S.; Soto, R.E.; Hornung, C.A.; Galandiuk, S. Smoking and inflammatory bowel disease: A meta-analysis. *Mayo Clin. Proc.* **2006**, *81*, 1462–1471. [CrossRef]
40. Dusabimana, T.; Park, E.J.; Je, J.; Jeong, K.; Yun, S.P.; Kim, H.J.; Kim, H.; Park, S.W. P2y2r deficiency ameliorates hepatic steatosis by reducing lipogenesis and enhancing fatty acid β-oxidation through ampk and pgc-1α induction in high-fat diet-fed mice. *Int. J. Mol. Sci.* **2021**, *22*, 5528. [CrossRef]
41. Ma, C.; Fu, Q.; Diggs, L.P.; McVey, J.C.; McCallen, J.; Wabitsch, S.; Ruf, B.; Brown, Z.; Heinrich, B.; Zhang, Q.; et al. Platelets control liver tumor growth through P2Y12-dependent CD40L release in NAFLD. *Cancer Cell* **2022**, *40*, 986–998.e5. [CrossRef]
42. Jain, S.; Pydi, S.P.; Jung, Y.H.; Scortichini, M.; Kesner, E.L.; Karcz, T.P.; Cook, D.N.; Gavrilova, O.; Wess, J.; Jacobson, K.A. Adipocyte P2Y14 receptors play a key role in regulating whole-body glucose and lipid homeostasis. *JCI Insight* **2021**, *6*, e146577. [CrossRef] [PubMed]

43. Das, S.; Seth, R.K.; Kumar, A.; Kadiiska, M.B.; Michelotti, G.; Diehl, A.M.; Chatterjee, S. Purinergic receptor X7 is a key modulator of metabolic oxidative stress-mediated autophagy and inflammation in experimental nonalcoholic steatohepatitis. *Am. J. Physiol.-Gastrointest. Liver Physiol.* **2013**, *305*, G950–G963. [CrossRef] [PubMed]
44. Chatterjee, S.; Rana, R.; Corbett, J.; Kadiiska, M.B.; Goldstein, J.; Mason, R.P. P2X7 receptor-NADPH oxidase axis mediates protein radical formation and Kupffer cell activation in carbon tetrachloride-mediated steatohepatitis in obese mice. *Free Radic. Biol. Med.* **2012**, *52*, 1666–1679. [CrossRef] [PubMed]
45. Liu, I.M.; Tzeng, T.F.; Tsai, C.C.; Lai, T.Y.; Chang, C.T.; Cheng, J.T. Increase in adenosine A1 receptor gene expression in the liver of streptozotocin-induced diabetic rats. *Diabetes/Metab. Res. Rev.* **2003**, *19*, 209–215. [CrossRef] [PubMed]
46. Grden, M.; Podgorska, M.; Szutowicz, A.; Pawelczyk, T. Diabetes-induced alterations of adenosine receptors expression level in rat liver. *Exp. Mol. Pathol.* **2007**, *83*, 392–398. [CrossRef]
47. Odashima, M.; Bamias, G.; Rivera-Nieves, J.; Linden, J.; Nast, C.C.; Moskaluk, C.A.; Marini, M.; Sugawara, K.; Kozaiwa, K.; Otaka, M.; et al. Activation of A2A adenosine receptor attenuates intestinal inflammation in animal models of inflammatory bowel disease. *Gastroenterology* **2005**, *129*, 26–33. [CrossRef]
48. Awad, A.S.; Huang, L.; Ye, H.; Duong, E.T.A.; Bolton, W.K.; Linden, J.; Okusa, M.D. Adenosine A2A receptor activation attenuates inflammation and injury in diabetic nephropathy. *Am. J. Physiol.-Ren. Physiol.* **2006**, *290*, F828–F837. [CrossRef]
49. Lukashev, D.; Ohta, A.; Apasov, S.; Chen, J.F.; Sitkovsky, M. Cutting edge: Physiologic attenuation of proinflammatory transcription by the Gs protein-coupled A2A adenosine receptor in vivo. *J. Immunol.* **2004**, *173*, 21–24. [CrossRef]
50. Cai, Y.; Li, H.; Liu, M.; Pei, Y.; Zheng, J.; Zhou, J.; Luo, X.; Huang, W.; Ma, L.; Yang, Q.; et al. Disruption of adenosine 2A receptor exacerbates NAFLD through increasing inflammatory responses and SREBP1c activity. *Hepatology* **2018**, *68*, 48–61. [CrossRef]
51. Zhou, J.; Li, H.; Cai, Y.; Ma, L.; Matthews, D.; Lu, B.; Zhu, B.; Chen, Y.; Qian, X.; Xiao, X.; et al. Mice lacking adenosine 2A receptor reveal increased severity of MCD-induced NASH. *J. Endocrinol.* **2019**, *243*, 199–209. [CrossRef]
52. Imarisio, C.; Alchera, E.; Sutti, S.; Valente, G.; Boccafoschi, F.; Albano, E.; Carini, R. Adenosine A 2a receptor stimulation prevents hepatocyte lipotoxicity and non-alcoholic steatohepatitis (NASH) in rats. *Clin. Sci.* **2012**, *123*, 323–332. [CrossRef]
53. Alchera, E.; Rolla, S.; Imarisio, C.; Bardina, V.; Valente, G.; Novelli, F.; Carini, R. Adenosine A2a receptor stimulation blocks development of nonalcoholic steatohepatitis in mice by multilevel inhibition of signals that cause immunolipotoxicity. *Transl. Res.* **2017**, *182*, 75–87. [CrossRef]
54. Peng, Z.; Borea, P.A.; Wilder, T.; Yee, H.; Chiriboga, L.; Blackburn, M.R.; Azzena, G.; Resta, G.; Cronstein, B.N. Adenosine signaling contributes to ethanol-induced fatty liver in mice. *J. Clin. Investig.* **2009**, *119*, 582–594. [CrossRef]
55. Figler, R.A.; Wang, G.; Srinivasan, S.; Jung, D.Y.; Zhang, Z.; Pankow, J.S.; Ravid, K.; Fredholm, B.; Hedrick, C.C.; Rich, S.S.; et al. Links between Insulin resistance, adenosine A2B receptors, and inflammatory markers in mice and humans. *Diabetes* **2011**, *60*, 669–679. [CrossRef]
56. Koupenova, M.; Johnston-Cox, H.; Vezeridis, A.; Gavras, H.; Yang, D.; Zannis, V.; Ravid, K. A 2b adenosine receptor regulates hyperlipidemia and atherosclerosis. *Circulation* **2012**, *125*, 354–363. [CrossRef]
57. Csóka, B.; Koscsó, B.; Töro, G.; Kókai, E.; Virág, L.; Németh, Z.H.; Pacher, P.; Bai, P.; Haskó, G. A2B Adenosine receptors prevent insulin resistance by inhibiting adipose tissue inflammation via maintaining alternative macrophage activation. *Diabetes* **2014**, *63*, 850–866. [CrossRef]
58. Johnston-Cox, H.; Koupenova, M.; Yang, D.; Corkey, B.; Gokce, N.; Farb, M.G.; LeBrasseur, N.; Ravid, K. The A2b adenosine receptor modulates glucose homeostasis and obesity. *PLoS ONE* **2012**, *7*, e40584. [CrossRef]
59. Suresh, R.R.; Jain, S.; Chen, Z.; Tosh, D.K.; Ma, Y.; Podszun, M.C.; Rotman, Y.; Salvemini, D.; Jacobson, K.A. Design and in vivo activity of A3 adenosine receptor agonist prodrugs. *Purinergic Signal.* **2020**, *16*, 367–377. [CrossRef]
60. Fishman, P.; Cohen, S.; Itzhak, I.; Amer, J.; Salhab, A.; Barer, F.; Safadi, R. The A3 adenosine receptor agonist, namodenoson, ameliorates non-alcoholic steatohepatitis in mice. *Int. J. Mol. Med.* **2019**, *44*, 2256–2264. [CrossRef]
61. Von Kügelgen, I.; Hoffmann, K. Pharmacology and structure of P2Y receptors. *Neuropharmacology* **2016**, *104*, 50–61. [CrossRef]
62. Caballero, F.; Fernández, A.; Matías, N.; Martínez, L.; Fucho, R.; Elena, M.; Caballeria, J.; Morales, A.; Fernández-Checa, J.C.; García-Ruiz, C. Specific contribution of methionine and choline in nutritional nonalcoholic steatohepatitis: Impact on mitochondrial S-adenosyl-L-methionine and glutathione. *J. Biol. Chem.* **2010**, *285*, 18528–18536. [CrossRef] [PubMed]
63. Kashireddy, P.V.; Rao, M.S. Lack of peroxisome proliferator-activated receptor α in mice enhances methionine and choline deficient diet-induced steatohepatitis. *Hepatol. Res.* **2004**, *30*, 104–110. [CrossRef] [PubMed]
64. Rizki, G.; Arnaboldi, L.; Gabrielli, B.; Yan, J.; Lee, G.S.; Ng, R.K.; Turner, S.M.; Badger, T.M.; Pitas, R.E.; Maher, J.J. Mice fed a lipogenic methionine-choline-deficient diet develop hypermetabolism coincident with hepatic suppression of SCD-1. *J. Lipid Res.* **2006**, *47*, 2280–2290. [CrossRef] [PubMed]
65. Mahi, N.A.; Najafabadi, M.F.; Pilarczyk, M.; Kouril, M.; Medvedovic, M. GREIN: An Interactive Web Platform for Re-analyzing GEO RNA-seq Data. *Sci. Rep.* **2019**, *9*, 7580. [CrossRef]
66. Kozumi, K.; Kodama, T.; Murai, H.; Sakane, S.; Govaere, O.; Cockell, S.; Motooka, D.; Kakita, N.; Yamada, Y.; Kondo, Y.; et al. Transcriptomics Identify Thrombospondin-2 as a Biomarker for NASH and Advanced Liver Fibrosis. *Hepatology* **2021**, *74*, 2452–2466. [CrossRef]

67. Nishiyama, K.; Aono, K.; Fujimoto, Y.; Kuwamura, M.; Okada, T.; Tokumoto, H.; Izawa, T.; Okano, R.; Nakajima, H.; Takeuchi, T.; et al. Chronic kidney disease after 5/6 nephrectomy disturbs the intestinal microbiota and alters intestinal motility. *J. Cell. Physiol.* **2019**, *234*, 6667–6678. [CrossRef]
68. Nishiyama, K.; Numaga-Tomita, T.; Fujimoto, Y.; Tanaka, T.; Toyama, C.; Nishimura, A.; Yamashita, T.; Matsunaga, N.; Koyanagi, S.; Azuma, Y.T.; et al. Ibudilast attenuates doxorubicin-induced cytotoxicity by suppressing formation of TRPC3 channel and NADPH oxidase 2 protein complexes. *Br. J. Pharmacol.* **2019**, *176*, 3723–3738. [CrossRef]